論文 **Original Paper**

Ternary boron-rich phases $AlMgB_{14}$ and $AlMgB_{22}$ grown from a molten Al–Mg–B mixture and properties of the crystals

Shigeru OKADA[1,a)], Kunio KUDOU[2], Takao MORI[3], Toetsu SHISHIDO[4] and Torsten LUNDSTRÖM[5]

Abstract: Crystals of ternary boron-rich phases $AlMgB_{14}$ and $AlMgB_{22}$ were grown from high-temperature Al–Mg–B ternary system solutions in an Ar atmosphere at 1673 K for 5 h. The optimum conditions for growing $AlMgB_{22}$ and $AlMgB_{14}$ were established using the starting mixtures of B/Mg = 0.5–1.0 and B/Mg = 2.0–6.0, respectively. The $AlMgB_{14}$ and $AlMgB_{22}$ crystals obtained have well-developed {001} and {100} faces, and were black color with a metallic luster. The maximum dimensions of $AlMgB_{14}$ and $AlMgB_{22}$ crystals were approximately 5.2 mm and 4.6 mm, respectively. The values of Vickers microhardness of $AlMgB_{14}$ and $AlMgB_{22}$ crystals are in the ranges of 23.9 ± 0.6 to 27.6 ± 0.6 GPa. The oxidation process of $AlMgB_{14}$ and $AlMgB_{22}$ crystals were studied below 1473 K by TG–DTA method. The susceptibility of $AlMgB_{14}$ does not show any particular features, with an increase at low temperatures indicative of a paramagnetic contribution, which is likely due to impurities. The susceptibility of the $AlMgB_{22}$ sample shows no apparent contribution from impurities and also does not have any anomalous behavior.

Keywords: $AlMgB_{14}$, $AlMgB_{22}$, Single crystal, Al–Mg–B ternary system solution, Vickers microhardness, Oxidation resistance, Magnetic susceptibility

1. Introduction

In the ternary Al–Mg–B system, two types of ternary structures, namely $AlMgB_{14}$ ($NaBB_{14}$-type) (orthorhombic, space group *Imam*) and $AlMgB_{22}$ (γ–AlB_{12}–type) (orthorhombic, space group $P2_12_12_1$) have been reported so far [1, 2]. Boron-rich compounds consisting of B_{12} icosahedra are of great interest of their remarkable physical and chemical properties, which in many cases are of potential interest for applications to thermoelectrics and photodetectors [3, 4]. However, there is very little information about the physicochemical and mechanical properties of $AlMgB_{14}$ and $AlMgB_{22}$. Crystals of aluminum magnesium borides are obtained by adding relatively large amount of Mg metal [3]. But, owing to the high vapour pressure of Mg at high temperature, optimum conditions for growing $AlMgB_{14}$ and $AlMgB_{22}$ crystals are not established.

The structure of the boron framework of $AlMgB_{14}$ is made up of four B_{12} icosahedra and eight isolated boron atoms per unit-cell (Fig. 1). Its structure is isotopic with $NaBB_{14}$-type (NaB_{15}) [5, 6] and $AlLiB_{14}$ [7], the metal atoms being distributed both in sites–I (4e positions), which are occupied by sodium in Na_xB_{15} phases and also in the smaller sites–II (1/4, 1/4, 1/4) which are empty in the case of sodium higher boride. Since aluminum atoms (r_{Al} = 0.143 nm) and magnesium atoms (r_{Mg} = 0.160 nm) are far smaller than sodium atoms (r_{Na} = 0.190 nm), there is a contraction of the unit-cell parameter in going from $NaBB_{14}$ (a = 0.5847 nm, b = 0.8415 nm, c = 1.0298 nm, V = 0.5067 nm^3) [6] to $AlMgB_{14}$ (a = 0.5848 nm, b = 0.8112 nm, c = 1.0312 nm, V = 0.4892 nm^3) [2]. Naslain et al. [6] and Higashi et al. [8] describe the mode of combination of these units in detail. The aluminum and magnesium atoms are accommodated in the large holes outside the icosahedra (Fig. 1). The occupancies of the metals are 75% and 78% for the Al and the Mg sites respectively, and the Mg site is split into two positions separated by 0.039 nm [8]. On the other hand, the structural analysis of $AlMgB_{22}$ (a = 1.6633 nm, b = 1.7547 nm, c = 1.0187 nm, V = 2.9731

[1] 工学部都市システム工学科，教授，工学博士
Department of Civil and Environmental Engineering, Faculty of Engineering; Professor, Dr. of Engineering; [a)]Corresponding author: Shigeru Okada, Tel/fax: +81–3–5481–3292,
E–mail address: shigeruokada@yahoo.co.uk (S. Okada)
[2] 神奈川大学，工学部機械工学科，専任講師，博士（工学）
Department of Mechanical Engineering, Faculty of Engineering, Kanagawa University; Lecturer, Dr. of Engineering, 3–27–1 Rokkakubashi, Kanagawa, Yokohama 221–8686
[3] 独立行政法人，物質・材料研究機構，研究員，理学博士
Advanced Materials Laboratory, National Institute for Materials Science, Research Worker, Dr. of Science; 1–1 Namiki, Tsukuba 305–0044
[4] 東北大学，金属材料研究所　新素材設計開発施設結晶作製研究ステーション，助教授，工学博士
Institute for Materials Research, Tohoku University, Associate Professor, Dr. of Engineering; 2–1–1 Katahira, Aoba, Sendai 980–0812
[5] スウェーデン国，ウプサラ大学，オングストローム研究所，教授，理学博士
The Ångström Laboratory, Inorganic Chemistry, Uppsala University, Professor, Dr. of Science; Box 538, SE–751 21 Uppsala, Sweden

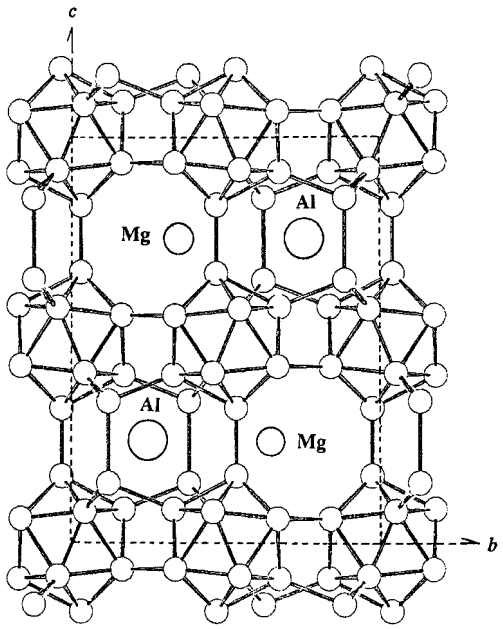

Fig. 1 The crystal structure of $AlMgB_{14}$ [8].

nm^3) revealed that the crystal has the same boron framework as γ–AlB_{12} [9, 10]. The Al and Mg atoms were distributed statistically over the eleven Al sites in the γ–AlB_{12} –type structure. Higashi [10] assume that the Al (4), Al (5) and Al (9) sites with relatively larger hole sizes than the rest (Al (1–3, 6–8, 10, 11)) were occupied by Mg atoms with a larger atomic size than Al. The occupational refinement based on that assumption led to the chemical $Al_{1.20}Mg_{0.47}B_{22}$, which is compatible with $Al_{1.40}Mg_{0.45}B_{22}$ obtained by chemical analysis.

In the present paper, we report the optimum experimental conditions for growing relatively large crystals of $AlMgB_{14}$ and $AlMgB_{22}$ from Mg metal and amorphous boron powders as the starting materials using an Al self-flux under an argon atmosphere. The size, morphology crystallographic data of the crystals were determined. Oxidation resistance in air up to 1473 K, Vickers microhardness, and magnetic susceptibility measurements at low temperatures of these compounds were studied.

2. Experimental details

The raw materials used were magnesium metal pieces (purity 99%), amorphous boron (purity 99.9%) and aluminum metal chips (purity 99.99%). Mg and B were weighed at nominal composition of atomic ratios B/Mg = 0.5–10.0 (Table 1), and Al metal was added to each mixture at a mass ratio of 1 : 15. The mixture was placed in a high dense Al_2O_3 crucible and heated in an argon atmosphere. The temperature of the furnace was raised to 1673 K, kept for 5 h and then cooled to room temperature at a rate of about 50 K·h^{-1}. The crystals were removed from the solidified melt by dissolving the matrix in dilute hydrochloric acid.

The crystal structures and unit-cell parameters of the phases were examined by the powder X-ray diffraction (XRD) with monochromatic CuK_α radiation and the Guinier-Hägg focusing X-ray powder diffraction camera (XDC–1000) with strictly monochromatic Cu$K_{\alpha 1}$ radiation. $AlMgB_{14}$ and $AlMgB_{22}$ crystals were selected under a stereomicroscope for the measurements of Vickers microhardness, oxidation resistance and magnetic susceptibility. The impurities content of the crystals were examined by a scanning electron microscope (SEM) equipped with an energy-dispersive detector (EDX).

The microhardness of the samples was measured at room temperature using a Vickers diamond pyramid as an indentor [11]. A load of 2.94 N was applied for 15 s and seven impressions were recorded for each sample. The obtained values were averaged and the experimental error was estimated. Thermogravimetric and differential thermal analyses (TG–DTA) were performed between room temperature and 1473 K to study the oxidation resistance of the samples in air. Pulverized samples of about 25 mg were heated at a rate of 10 K·min^{-1}. The oxidation products were analyzed by XRD. Magnetic susceptibility of $AlMgB_{14}$ and $AlMgB_{22}$ was measured by using a commercial superconducting quantum interference device

Table 1 Growth conditions of $AlMgB_{14}$ and $AlMgB_{22}$ crystals obtained using magnesium metal and amorphous boron powders as the starting materials in an Al solution.

Run no.	Composition of the starting material (atomic ratio) Mg	B	Soaking temp. (K)	Soaking time (h)	Phases identified
1	1	0.5	1673	5	$AlMgB_{22}$, α–AlB_{12}, AlB_2, $AlMgB_{14}$
2	1	1.0	1673	5	$AlMgB_{22}$, α–AlB_{12}, AlB_2, $AlMgB_{14}$
3	1	2.0	1673	5	$AlMgB_{14}$, AlB_2, $AlMgB_{22}$, α–AlB_{12}
4	1	4.0	1673	5	$AlMgB_{14}$, AlB_2, α–AlB_{12}, $AlMgB_{22}$
5	1	5.0	1673	5	$AlMgB_{14}$, AlB_2, α–AlB_{12}, $AlMgB_{22}$
6	1	6.0	1673	5	$AlMgB_{14}$, α–AlB_{12}, AlB_2, $AlMgB_{22}$
7	1	8.0	1673	5	α–AlB_{12}, AlB_2, $AlMgB_{14}$, $AlMgB_{22}$
8	1	10.0	1673	5	α–AlB_{12}, AlB_2, $AlMgB_{14}$, $AlMgB_{22}$

Al metal was added to each mixture at a mass ratio of 1 : 15.

(SQUID) magnetometer in the temperature range of 2 K to 300 K.

3. Results and discussion

3.1. Crystal growth of $AlMgB_{14}$ and $AlMgB_{22}$

The results of the phase analysis are listed in Table 1. As seen from Table 1, four types of structures, namely AlB_2, α–AlB_{12}, $AlMgB_{14}$ and $AlMgB_{22}$ were identified, while crystals of γ–AlB_{12} and MgB_2 were not detected by XRD.

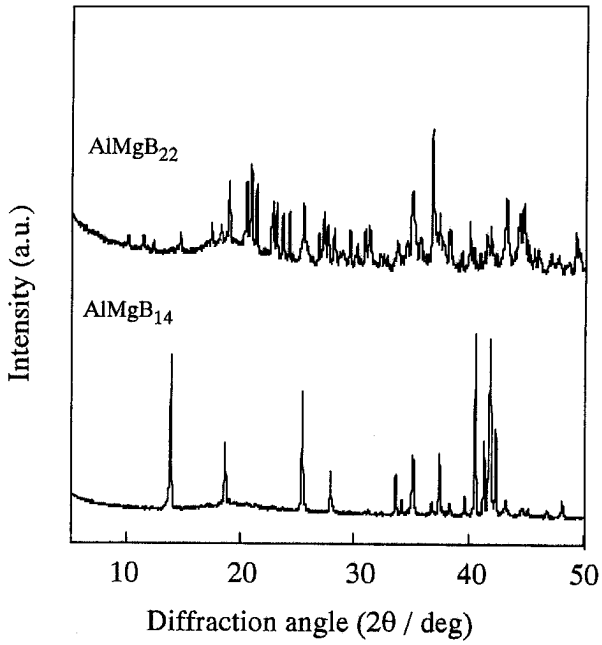

Fig. 2 Powder XRD patterns of $AlMgB_{14}$ and $AlMgB_{22}$ crystals.

Variation of the atomic ratio of the starting materials gave different products. The optimum conditions for growing $AlMgB_{22}$ and $AlMgB_{14}$ were established using the starting mixtures of B/Mg = 0.5–1.0 (Run no. 1 and 2) and B/Mg = 2.0–6.0 (Run no. 3–6). Fig. 2 shows the XRD patterns of $AlMgB_{14}$ and $AlMgB_{22}$ crystals. The $AlMgB_{14}$ and $AlMgB_{22}$ crystals obtained have well-developed {001} and {100} faces, and were black color with a metallic luster (Fig. 3). The maximum dimensions of $AlMgB_{14}$ and $AlMgB_{22}$ crystals were approximately 5.2 mm and 4.6 mm, respectively. The basic crystal data of $AlMgB_{14}$ and $AlMgB_{22}$ crystals are listed in Table 2. The unit-cell parameters of these compounds are in relatively good agreement with data published previously [1, 2]. Although the impurity content of the $AlMgB_{14}$ and $AlMgB_{22}$ crystals was not analyzed chemically, the EDX established the occurrence of traces of calcium and iron elements.

3.2. Properties

The values of Vickers microhardness of $AlMgB_{14}$ and $AlMgB_{22}$ crystals are listed in Table 3. The values of $AlMgB_{14}$ are in the ranges of 23.9 ± 0.6, 25.5 ± 0.5 and 27.6 ± 0.6 GPa for {100}, {010} and {001} faces, respectively. The values measured on {010} faces of the crystals are in comparatively good agreement with the values of these faces for $AlMgB_{14}$ in the literature [2]. However, the value measured on the {001} face of $AlMgB_{14}$ is in the range of 27.6 ± 0.6 GPa, which is relatively higher than that observed on the {100} and {010} faces. This anisotropic nature of hardness seems to be related to the difference in the number of B_{12} icosahedra units and B–B bonds for linkage of boron atoms in the structures. On the other hand, the value of $AlMgB_{22}$ is in the range of $25.4 \pm$

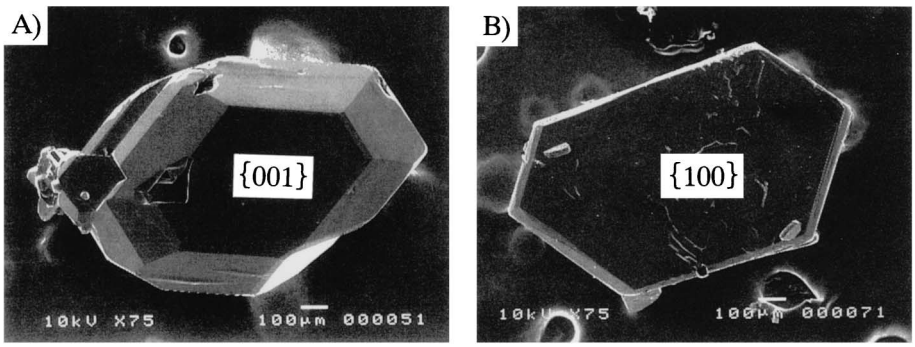

Fig. 3 SEM micrographs of $AlMgB_{14}$ crystal (A) (Run no. 4) and $AlMgB_{22}$ crystal (B) (Run no. 2).

Table 2 Unit–cell parameters of $AlMgB_{14}$ and $AlMgB_{22}$ crystals.

Formula unit	Space group	Unit–cell parameter (nm)			V (nm^3)	Ref.
		a	b	c		
$AlMgB_{14}$	*Imam*	0.58450(2)	0.81137(7)	1.03298(4)	0.4899(1)	This work
$AlMgB_{14}$	*Imam*	0.5848(1)	0.8112(1)	1.0312(1)	0.4892(1)	[2]
$AlMgB_{22}$	$P2_12_12_1$	1.66243(8)	1.75537(8)	1.01639(4)	2.9660(1)	This work
$AlMgB_{22}$	$P2_12_12_1$	1.6633(3)	1.7547(4)	1.0187(2)	2.9731(2)	[1]

Table 3 Vickers microhardness of $AlMgB_{14}$ and $AlMgB_{22}$ crystals.

Compound	indentation plane	Hardness (GPa)	Ref.
$AlMgB_{14}$	{001}	27.6±0.6	This work
	{010}	25.5±0.5	This work
	{100}	23.9±0.6	This work
	{001}	27.7±0.5	[2]
$AlMgB_{22}$	{100}	25.4±0.5	This work

Table 4 Results of the TG–DTA measurements for $AlMgB_{14}$ and $AlMgB_{22}$ crystals.

Compounds	Oxidation start (K)	Exothermic maximum (K)	Weight gain (mass%)	Oxidation products
$AlMgB_{14}$	920	1327, 1419	16.9	B_2O_3, $Al_4B_2O_9$
$AlMgB_{22}$	930	1421	9.6	—

0.5 GPa for {100} face.

The oxidation process of $AlMgB_{14}$ and $AlMgB_{22}$ crystals were studied below 1473 K by TG–DTA method, as shown in Fig. 4. The oxidation of $AlMgB_{14}$ and $AlMgB_{22}$ crystals began to proceed at approximately 920 and 930 K, respectively. The weight gain of the compounds after heating in air up to 1473 K is 16.9 and 9.6%, respectively. $AlMgB_{22}$ show relatively high oxidation resistance. The final oxidation products of $AlMgB_{14}$ include B_2O_3 and $Al_4B_2O_9$, and so the exothermic peaks are attributed to oxidation products. However, oxidation product of $AlMgB_{22}$ crystal was not detected from XRD, probably due to insufficient amounts of this oxidation product. The results of TG–DTA are listed in Table 4.

Recently, interesting magnetic behavior has been observed in B_{12} icosahedra compounds like REB_{50} (RE = rare earth) [12] and TbB_{25} [13]. It was indicated that the magnetic interaction is mediated by the B_{12} icosahedra [12], which is a completely new phenomena in boride compounds. Although there are no atoms with large magnetic spin among the $AlMgB_{14}$ and $AlMgB_{22}$ [14] compounds, it is important to characterize the magnetic properties of these new B_{12} compounds, of which $AlMgB_{14}$ has a structure similar to TbB_{25} [13], since the magnetic properties have been completely unknown to date. The temperature dependence of the magnetic susceptibility of $AlMgB_{14}$ and $AlMgB_{22}$ compounds was measured down to 2 K and is shown in Fig. 5. The susceptibility of $AlMgB_{14}$ does not show any particular features, with an increase at low temperatures indicative of a paramagnetic contribution, which is likely due to impurities. The susceptibility of the $AlMgB_{22}$ sample shows no apparent contribution from impurities and also does not have any anomalous behavior.

4. Conclusion

The single crystals of the ternary borides $AlMgB_{14}$ and

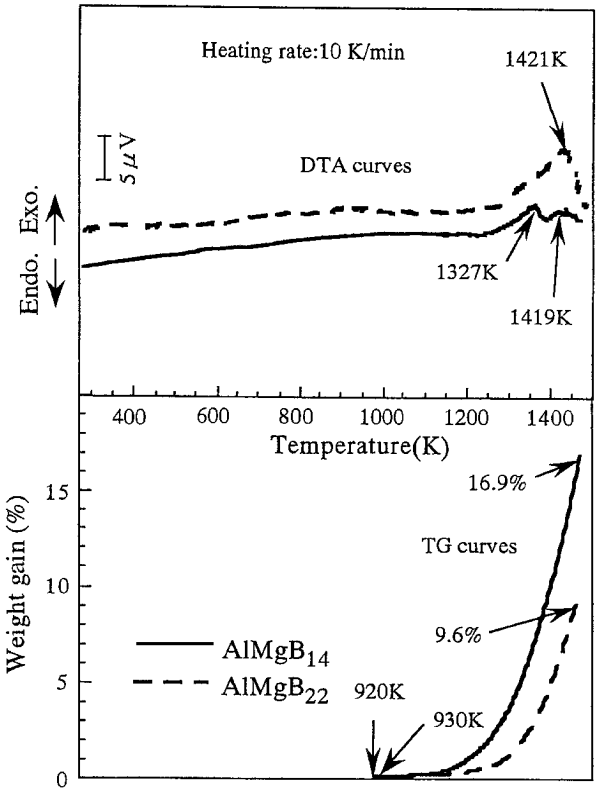

Fig. 4 TG–DTA curves for $AlMgB_{14}$ and $AlMgB_{22}$ heated in air.

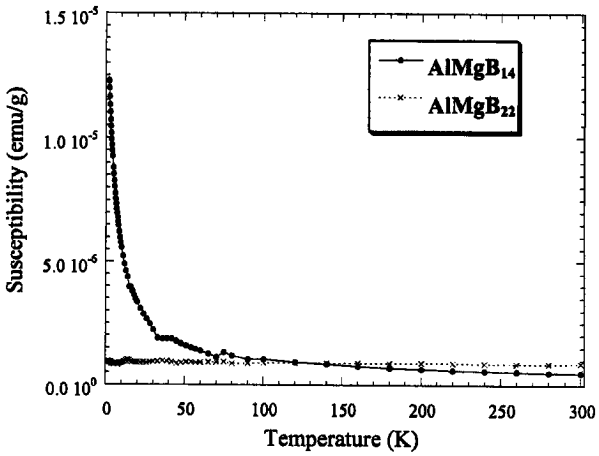

Fig. 5 Temperature dependence of the magnetic susceptibility of $AlMgB_{14}$ and $AlMgB_{22}$ crystals.

$AlMgB_{22}$ have been grown from high-temperature Al–Mg–B ternary system solutions using Mg metal and amorphous B powders as starting materials under an Ar atmosphere at 1673 K for 5 h. The growth conditions for large crystals of $AlMgB_{14}$ and $AlMgB_{22}$ were established. The $AlMgB_{14}$ and $AlMgB_{22}$ crystals obtained have well-developed {001} and {100} faces, and were black color with a metallic luster. The results of measurements of the unit-cell parameters determined are as follows: for $AlMgB_{14}$, $a = 0.58450(2)$ nm, $b = 0.81137(7)$ nm, $c = 1.03298(4)$ nm, $V = 0.4899(1)$

nm^3; for $AlMgB_{22}$, $a = 1.66243(8)$ nm, $b = 1.75537(8)$ nm, $c = 1.01639(4)$ nm, $V = 2.9660(1)$ nm^3. The values of Vickers microhardness of the $AlMgB_{14}$ and $AlMgB_{22}$ crystals are in the ranges of 23.9 ± 0.6 to 27.6 ± 0.6 GPa. The TG curves show that the oxidation of $AlMgB_{14}$ and $AlMgB_{22}$ crystals start at approximately 920 and 930 K, respectively. The results of magnetic susceptibility measurements at low temperatures of the compounds are discussed.

Acknowledgements

The authors would like to thank Dr. K. Iizumi, Dr. M. Ogawa, Miss Y. Igumi and Miss N. Suzuki of Tokyo Polytechnic University for their help in the experiments.

References

[1] I. Higashi, M. Kobayashi, Y. Takahashi, S. Okada and K. Hamano, J. Crystal Growth, **99** (1990) 998–1004.

[2] I. Higashi, M. Kobayashi, S. Okada, K. Hamano and T. Lundström, J. Crystal Growth, **128** (1993) 1113–1119.

[3] V. I. Matkovich ed., "*Boron and Refractory Borides*", Spring-Verlag, New York, 1977, pp. 439–pp. 445.

[4] H. Werheit, U. Kuhlmann, G. Krach, I. Higashi, T. Lundström and Y. Yang, J. Alloys Compd., **202** (1993) 269–281.

[5] V. I. Matkovich and J. Economy, Acta Cryst., **B26** (1970) 616–621.

[6] R. Naslain, A. Guette and P. Hagenmuller, J. Less-Common Metals, **47** (1976) 1–16.

[7] K. Kudou, S. Okada, T. Mori, K. Iizumi, T. Shishido, T. Tanaka, I. Higashi, K. Nakajima, P. Rogl, Y. B. Adnersson and T. Lundström, Jpn. J. Appl. Phys., **41** (2002) L928–L930.

[8] I. Higashi and T. Ito, J. Less-Common Metals, **92** (1983) 239–246.

[9] R. E. Hughes, M. E. Leonowicz, J. L. Lemley and L.-T. Tai, J. Am. Chem. Soc., **99** (1977) 5507–5512.

[10] I. Higashi, J. Solid State Chem., **24** (1983) 333–338.

[11] S. Okada, K. Kudou, T. Tanaka, T. Shishido, V–N. Gurin and T. Lundström, J. Solid State Chem., **177**, 547–550 (2004).

[12] T. Mori and T. Tanaka, J. Phys. Soc. Jpn., **68**, 2033–2039 (1999).

[13] T. Mori, F. Zhang, and T. Tanaka, J. Phys.: Condens. Matter, **13**, L423–L430 (2001).

[14] S. Okada, K. Kudou, T. Mori, T. Shishido, I. Higashi, N. Kamegashira, K. Nakajima and T. Lundström, Designing, Processing and Properties of Advanced Engineering Materials, in press (2004).